Scientific paper

Amperometric Biosensor for Xanthine Determination Based On Fe_3O_4 Nanoparticles

Funda Özcan Öztürk,[1] Pınar Esra Erden,[2,*] Ceren Kaçar[2] and Esma Kiliç[2]

[1] *Namık Kemal University, Faculty of Arts and Science, Department of Chemistry, Tekirdağ, Turkey*

[2] *Ankara University, Faculty of Science, Department of Chemistry, Ankara, Turkey*

** Corresponding author: E-mail: erdenpe@gmail.com*
Tel No.: +90(312)2126720/1278; Fax No.: +90(312)2232395

Received: 06-06-2013

Abstract

An amperometric xanthine biosensor was developed based on the immobilization of xanthine oxidase (XO) into the Fe_3O_4 nanoparticles modified carbon paste. Electron transfer properties of unmodified and Fe_3O_4 nanoparticles modified carbon paste electrodes were investigated by cyclic voltammetry and electrochemical impedance spectroscopy. Fe_3O_4 nanoparticles increased electroactive surface area of the electrode and electron transfer at solution/electrode interface. Optimum pH, nanoparticle loading and enzyme loading were found to be 6.0; 14.2% and 0.6 Unit XO respectively. Fe_3O_4 nanoparticles modified carbon paste enzyme electrode allowed xanthine determination at –0.20 V, thus minimizing the potential interferences from electrochemically oxidizable substances such as ascorbic acid and uric acid. A linear relationship was obtained in the concentration range from 7.4×10^{-7} mol L^{-1} to 7.5×10^{-5} mol L^{-1} and a detection limit of 2.0×10^{-7} mol L^{-1}. The biosensor was used for determination of xanthine in urine samples and the results indicate that the biosensor is effective for the detection of xanthine.

Keywords: Xanthine; Amperometry; Biosensor; Fe_3O_4 nanoparticles; Carbon paste

1. Introduction

Xanthine (3,7-dihydro-1H-purine-2,6-dione) is a purine base found in most human body tissues and fluids and in other organisms. Xanthine is generated from guanine by guanine deaminase and from hypoxanthine by xanthine oxidase. In clinical diagnostics, the concentration of xanthine in blood and urine is used as an indicator for certain pathologies such as xanthinuria, renal failure and gout.[1–3] Xanthine concentration is also used as an index for evaluating the fish freshness in food industry.[4] Thus, rapid, accurate, sensitive and selective determination of xanthine is of considerable importance in clinical analysis and food quality control. Various techniques have been utilized to determine xanthine including capillary column gas chromatography,[5] HPLC,[6] capillary electrophoresis-electrochemical analyses,[7] chemiluminesence,[8] spectrophotometry.[9] However, such detection are often complicated, expensive, time-consuming and require sample preparation and are not suitable for real time monitoring. Biosensors allow direct, rapid and inexpensive measurement of xanthine in samples.

Xanthine oxidase (EC.1.1.3.22) is a complex metal containing flavoprotein catalyzing the oxidation of hypoxanthine to xanthine and further catalyzing the oxidation of xanthine to uric acid according to the following equations:[10]

$$\text{Hypoxanthine} + O_2 \xrightarrow{\text{xo}} \text{Xanthine} + H_2O_2$$

$$\text{Xanthine} + O_2 \xrightarrow{\text{xo}} \text{Uric acid} + H_2O_2$$

Amperometric determination of xanthine or hypoxanthine is mainly based on the electrooxidation of hydrogen peroxide and/or uric acid generated by xanthine oxidase using positive detection potentials.[11–13] However, high potentials applied to the working electrode make the biosensor responsive to other electroactive substances such as ascorbic acid and uric acid. In order to eliminate the effect of interferences and to enhance the selectivity of the biosensor, use of electron transfer mediators such as ferrocene,[14] Prussian blue,[10,15] colloidal gold,[10] cobalt phthalocyanine and ferricyanide[16] was reported in xanthi-

ne or hypoxanthine biosensors. Xanthine determination based on electroreduction of H_2O_2 at working potentials of about 0 V can also be used for the interference-free sensing of xanthine.[17] Another approach to lower the working potential is the use of HRP together with xanthine oxidase and perform xanthine determination via H_2O_2 reduction.[18] In xanthine and hypoxanthine biosensors use of polyelectrolyte multilayer films[19] or nafion coatings[20] to improve the selectivity was also reported.

Recently, nanostructure metal oxides have found numerous applications in biosensors due to their unique chemical and physical properties such as large surface area, high surface reaction activity, high catalytic efficiency, chemical stability and strong adsorption ability. Among the various metal oxide nanoparticles magnetite nanoparticles have been exploited as a potential material for biosensing due to their superior characteristics like biocompatibility, strong superparamagnetic property and low toxicity.[21–25] The major goal of our work was to develop and investigate a simple, low-cost and high performance electrochemical biosensor for xanthine determination, based on carbon paste electrode modified with Fe_3O_4 nanoparticles and xanthine oxidase. In this work, we investigated the parameters that influence the electrode performance, the analytical characteristics and the use of the enzyme electrode for xanthine determination in real samples.

2. Experimental

The electrochemical studies were carried out with IVIUM electrochemical analyzer (Ivium Technologies, Netherlands) and a three-electrode cell stand (Bioanalytical Systems, Inc., USA). The working electrode was a modified carbon paste electrode. The counter and the reference electrodes were a Pt wire (BAS MW 1034) and Ag/AgCl (BAS MF 2052) electrode, respectively (Bioanalytical Systems, Inc., USA). The pH values of the buffer solutions were measured with ORION Model 720A pH/ion meter and ORION combined pH electrode (Thermo Scientific, USA). All aqueous solutions were prepared with double-distilled deionized water supplied from Human Power I+, Ultra Pure Water System (Produced by ELGA as PURELAB Option-S).

Xanthine oxidase (E.C. 3.5.3.3 from *Arthrobacter* sp. with a specific activity of 8.7 Units/mg solid), Fe_3O_4 nanoparticles (<50 nm), uric acid, ascorbic acid and glutaraldehyde were purchased from Sigma (St. Louis, MO, USA). Sodium monohydrogenphosphate and sodium dihydrogenphosphate were supplied from Riedel-de Haën (Seelze, Germany). Xanthine, bovine serum albumin (BSA), graphite powder, paraffin oil and glucose were from Fluka (Buchs, Switzerland). All other chemicals were obtained from Merck (Darmstadt, Germany). Standard solutions of xanthine were prepared freshly every day by dissolving xanthine in water with 0.1 mol L^{-1} NaOH.

Carbon paste was prepared in the following proportions for unmodified electrode (UCPE): 77.6% graphite powder and 22.4% paraffin oil. Fe_3O_4 nanoparticles modified carbon paste electrode (Fe_3O_4–CPE) was composed of 63.4% graphite powder, 14.2% Fe_3O_4 nanoparticles and 22.4% paraffin oil. The modified electrode was prepared by hand-mixing graphite powder with the nanoparticles and then adding paraffin oil and throughly mixing for approximately 20 minutes to form homogeneous modified carbon paste electrode.

Graphite powder and Fe_3O_4 nanoparticles were mixed and enzyme solution (24 μL xanthine oxidase (25.1 Unit/mL), 1.5 mg BSA and 10 μL 1.25% glutaraldehyde) was added for Fe_3O_4 nanoparticles modified enzyme electrode (Fe_3O_4–CPEE) construction. Paraffin oil was added after the evaporation of water and mixed for approximately 20 minutes until a uniform paste was obtained. In all cases, the paste was placed into the bottom of the working electrode body and the electrode surface was polished with a weight paper to have a smooth surface. The stepwise fabrication processe of the modified electrode is presented in Scheme 1. The electrodes were only washed with water and working buffer between

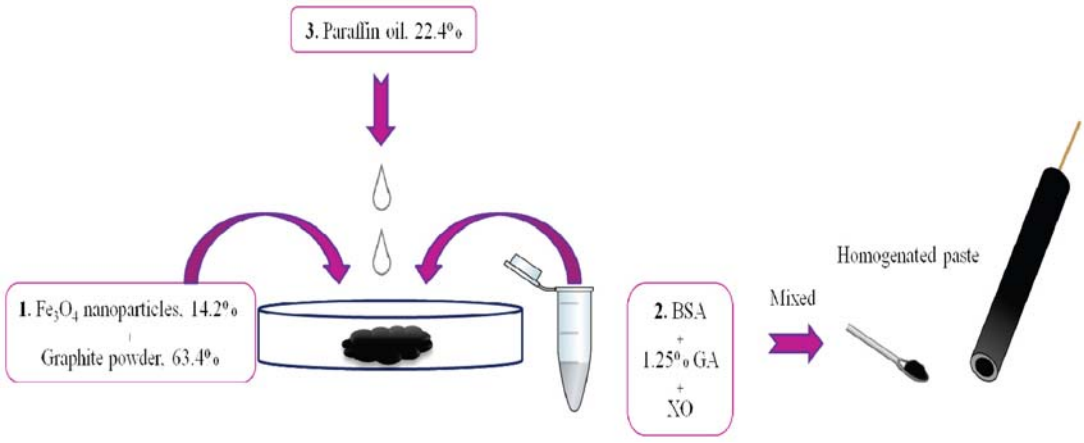

Scheme 1. The stepwise fabrication processes of the modified electrode

measurements. Electrodes were stored in refrigerator at +4 °C when not in use.

Electron transfer properties of unmodified and modified electrodes were examined in 0.1 mol L^{-1} KCl solution containing 5 mmol L^{-1} $K_3[(Fe(CN)_6]$ + 5 mmol L^{-1} $K_4[(Fe(CN)_6]$ by cylic voltammetry and electrochemical impedance spectroscopy. The cyclic voltammograms of UCPE and Fe_3O_4–CPE were recorded between (–0.5)V–(+1.0)V. Electrochemical impedance spectroscopy measurements were performed at the frequency range of 10^5–0.05 Hz with 10 mV amplitude under open circuit potential (E_{OCP}) conditions. All other amperometric measurements were performed in phosphate buffer solution (0.05 mol L^{-1} pH 6.0). Measurements were carried out at room temperature (23 ± 2 °C).

3. Results and Discussion

3. 1. Electrochemical Characterization of Unmodified and Modified Electrodes Without Enzyme

The cyclic voltammograms of the UCPE and Fe_3O_4–CPE are shown in Fig. 1. Well-defined oxidation and reduction peaks of $Fe(CN)_6^{3-/4-}$ were observed at the unmodified carbon paste electrode. After the electrode was modified with Fe_3O_4 it was observed that Fe_3O_4 nanoparticles increased peak current and decreased peak-to-peak separation ($E_{p,a} - E_{p,c} = \Delta E_p$) for $Fe(CN)_6^{3-/4-}$ waves. The ΔE_p for UCPE and Fe_3O_4–CPE were found as 390 mV and 270 mV, respectively. The voltammetric study suggests that the presence of Fe_3O_4 nanoparticles results in increased electroactive surface area and enhanced electron transfer.[26,27] The electrochemical surface area of Fe_3O_4–CPE was calculated from the voltammetric peak current by the use of the Randles-Sevcik equation.[28,29] The effective electrochemical surface area of Fe_3O_4–CPE (0.197 cm^2) is much higher than the surface area of the UCPE (0.123 cm^2). It can be concluded that the higher surface area will enhance the sensitivity of electrode.

Electrochemical impedance spectroscopy of $[Fe(CN)_6]^{4-/3-}$ solution is a valuable technique to give information on impedance changes of the electrode surface in the modification process. In Nyquist plots the imaginary impedance (Z") is plotted against the real impedance (Z'). Fig. 2 exhibits the electrochemical impedance spectra of UCPE and Fe_3O_4–CPE. The Nyquist plot of impedance spectra includes a semicircle portion and a linear portion. The semicircle portion at high frequencies corresponds to the electron transfer limited process, and the linear portion at low frequencies corresponds to the diffusion process. The diameter of the semicircles is equal to the electron transfer resistance at the electrode surface (R_{ct}).[22,30] The R_{ct} of UCPE was much larger than Fe_3O_4–CPE indicating that Fe_3O_4 nanoparticles have good conductivity and enhance electron transfer efficiency at solution/electrode interface. The higher electron transfer efficiency can promote the electroreduction of enzymatically produced H_2O_2.

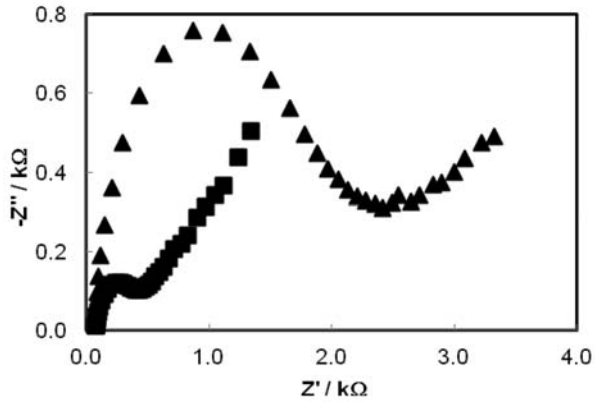

Fig. 2. The Nyquist curves of (▲) UCPE and (■) Fe_3O_4–CPE in 0.1 mol L^{-1} KCl solution containing 5 mmol L^{-1} $Fe(CN)_6^{3-/4-}$

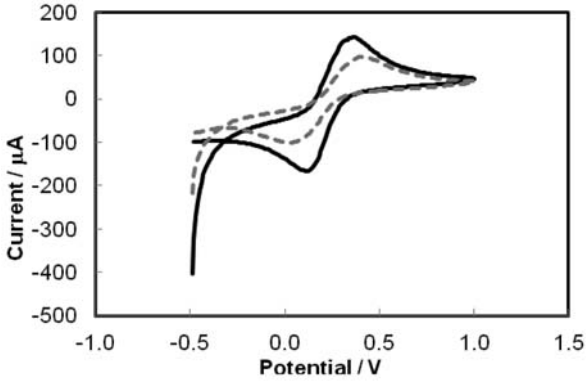

Fig. 1. Cyclic voltammograms of UCPE (dashed line), Fe_3O_4–CPE (solid line) at 50 mVs^{-1}, in 0.1 mol L^{-1} KCl solution containing 5 mmol L^{-1} $Fe(CN)_6^{3-/4-}$

3. 2. Xanthine Responses of Carbon Paste and Modified Carbon Paste Enzyme Electrodes

The quantification of xanthine is based on the electrochemical detection of the enzymatically produced H_2O_2, the sensitivity of the electrode is dependent on the electrochemical response to H_2O_2. Electrodes with high catalytic efficiency to H_2O_2 would achieve high sensitivity to xanthine. Thus, the H_2O_2 response of the unmodified and modified electrodes prepared without enzyme was firstly investigated. Fig. 3 shows the current difference values versus H_2O_2 concentration obtained with UCPE and Fe_3O_4–CPE at –0.20 V versus Ag/AgCl. It is clear from the figures that the sensitivity of the Fe_3O_4–CPE (y =

1.76x + 0.086, R^2 = 0.9955) is higher than that of unmodified carbon paste electrode (y = 0.34x + 0.003, R^2 = 0.9943) to H_2O_2. From these results, it can be concluded that Fe_3O_4 nanoparticles increased catalytic activity toward electrochemical reduction of H_2O_2.

After determining the catalytic activity of nanoparticles, Fe_3O_4–CPE was modified with enzyme. The xanthine response of the modified enzyme electrode (Fe_3O_4–CPEE) in nitrogen saturated buffer solution was determined and compared with that obtained in oxygen saturated solution to clarify the detection mechanism of the purposed biosensor. Fe_3O_4–CPEE showed very small catalytic activity towards xanthine in nitrogen saturated solution in contrast to the response in oxygen saturated solution. This indicates that Fe_3O_4 nanoparticles cannot efficiently catalyse the electron transfer between the reduced enzyme and electrode surface. It can be concluded that Fe_3O_4 nanoparticles do not show a good mediating capability. Fe_3O_4 nanoparticles with the valance state of Fe(II) and Fe(III) was reported as the catalyst for H_2O_2 detection.[26,31] According to this, we can conclude that in our study Fe_3O_4 nanoparticles as a catalyst are very efficient for the electrocatalytic reduction of hydrogen peroxide, can enhance the current response of the enzyme electrode and as a result increase the sensitivity of the biosensor.[26,32]

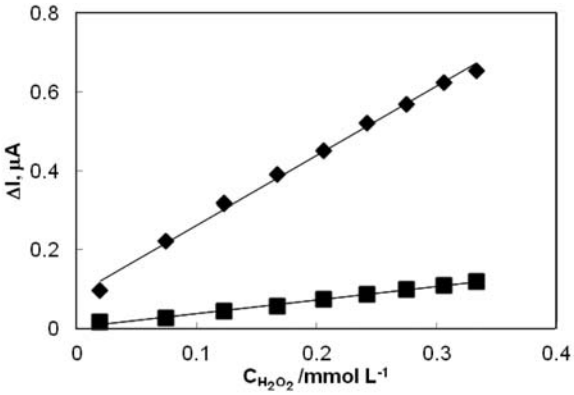

Fig. 3. Calibration curves for H_2O_2: (◆)UCPE, (■) Fe_3O_4–CPE (0.05 mol L^{-1} pH 6.0 phosphate buffer, –0.20 V)

3. 3. Optimum Working Conditions and Electrode Composition of Fe_3O_4–CPEE

The sensitivity and stability of the enzyme electrodes constructed without BSA and glutaraldehyde were investigated. Fe_3O_4 modified carbon paste enzyme electrodes were constructed using three different immobilization procedures. The enzyme directly incorparated into carbon paste was tested as the first immobilization procedure. The enzyme mixed with glutaraldehyde and incorporated into carbon paste matrix was tested as the second immobilization procedure. Finally enzyme was immobilized into carbon paste matrix by crosslinking with BSA and glutaraldehyde. The enzyme electrode constructed with xanthine oxidase, BSA and glutaraldehyde showed the best sensitivity and stability. Thus, this immobilization procedure was selected as the optimum one and used for the construction of the enzyme electrode. It is probable that crosslinking with BSA and glutaraldehyde prevents the enzyme leaking out of the carbon paste matrix resulting in a higher sensitivity and operational stability. Similar behaviour was also reported in the literature.[11,33]Agui et al., evaluated different electrode compositions for the construction of hypoxanthine biosensors and reported that the enzyme electrode in which xanthine oxidase was immobilized by crosslinking with glutaraldehyde and BSA showed the highest signal for hypoxanthine.[11] Zhang et al., studied the effect of BSA on the sensitivity of uric acid biosensor. It was reported that the sensitivity of the biosensor without BSA was three times less sensitive than that of a biosensor with BSA. The authors suggested that BSA can entrap larger amounts of uricase and thus enhance the immobilization of enzymes.[33]

The amperometric response of an enzyme electrode greatly depends on the amount of the enzyme loaded. Thus, the effect of the enzyme loading in carbon paste matrix on the response was investigated. The response of the Fe_3O_4–CPEE was measured at four different enzyme amounts as 0.4, 0.6, 0.8 and 1.0 Units by keeping the other parameters constant. The highest sensitivity was observed at the loading of 0.6 Units as can be seen in Fig. 4(A). The linearities and the working ranges of the calibration graphs recorded for electrodes containing 0.4, 0.8 and 1.0 Units enzyme were not satisfactory.

A study was carried out to evaluate the effect of nanoparticle amount on the electrode response. Fe_3O_4 amount was varied as 7.8%, 10.3%, 14.2% and 15.5% while the graphite and paraffin oil amount kept constant. Fig. 4 (B) shows the sensitivities obtained with different amounts of nanoparticle. The highest sensitivity and working range was obtained with the carbon paste electrodes with 14.2% Fe_3O_4.

The performance of an enzyme electrode strongly depends on the pH value, because the acidity of the working solution has a significant effect on the redox behaviour of the enzymes.[34] The dependence of enzymatic activity of the immobilized XO on pH was investigated in order to find the optimal pH for the xanthine enzyme electrode. This study was carried out at 0.1 mmol L^{-1} xanthine concentration over the pH range from 5.5 to 8.0 (Fig. 4(C)). The response current increases with increasing pH from 5.5 to 6.0 and then decreases as pH increases further. The highest response was obtained at pH 6.0. Therefore, pH 6.0 was selected in the subsequent experiments. Different pH values such as; pH 5.5,[36] pH 6.8,[19] pH 7.0,[12,35,37] pH 7.4,[16] pH 7.5,[18] pH 8.5[38] were also reported in the literature for xanthine oxidase based enzyme electrodes. This can be attributed to the fact that the enzyme supply, im-

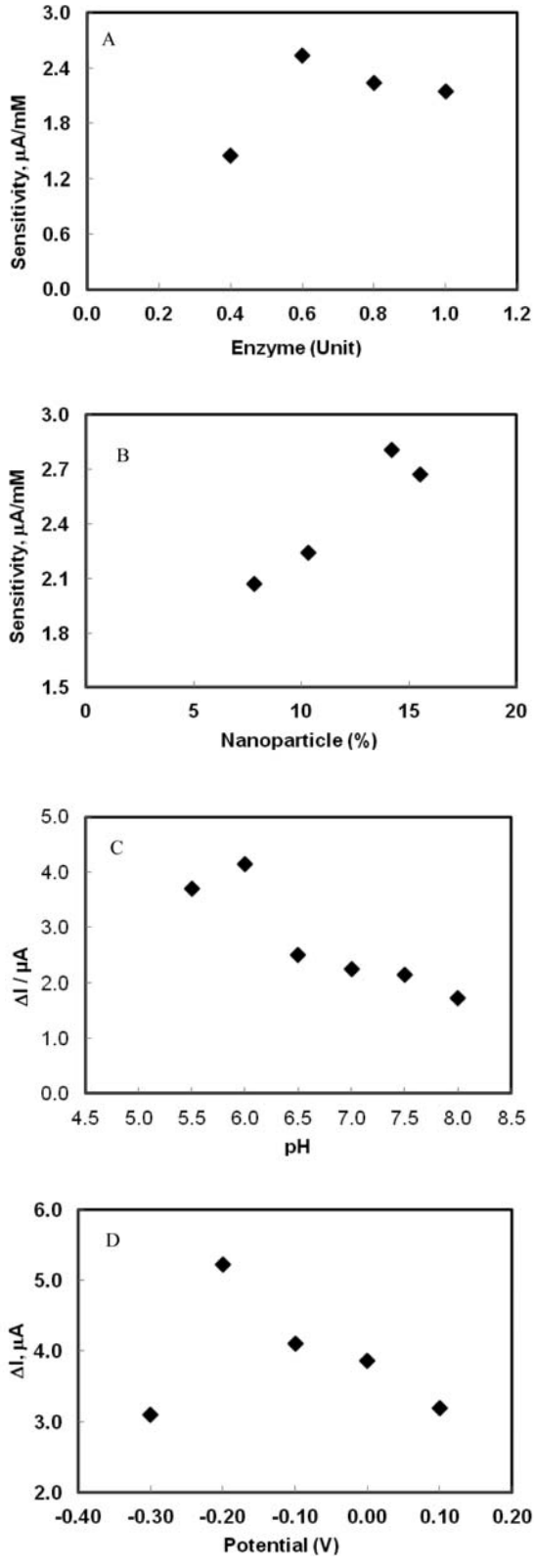

Fig. 4. (A) The effect of enzyme loading on the response of Fe_3O_4–CPEE (B) The effect of nanoparticle amount on the response of Fe_3O_4–CPEE (0.05 mol L^{-1} pH 6.0 phosphate buffer,–0.20 V) (C) The effect of buffer pH on the response of Fe_3O_4–CPEE (0.05 mol L^{-1} phosphate buffer,–0.20 V) (D) The effect of working potential on the response of Fe_3O_4–CPEE (0.05 M pH 6.0 phosphate buffer)

mobilization method and electrode preparation procedures were different. The decrease in the response of the enzyme electrode at pH values below and above 6.0 may be resulted from the change of the enzyme conformations leading to a decrease in the enzyme activity.

The applied potential has critical role in biosensor applications. In this study the effect of applied potential on the enzyme electrode was investigated between (–0.30) V – (+0.10) V in the presence of 0.1 mmol L^{-1} xanthine. The amperometric response increased as the applied potential shifted from –0.30 V to –0.20 V and then decreased at potentials more than –0.10 V (Fig. 4D). Therefore, –0.20 V which exhibited the highest current was selected as the optimum potential. A working potential of –0.20 V is also important to minimize possible the interferences at determination of xanthine.

3. 4. Performance Parameters of Fe_3O_4–CPEE

Fig. 5 shows the amperometric response curve of the Fe_3O_4–CPEE recorded as a function of xanthine concentration under the optimized experimental conditions. The response current increases with the increasing xanthine concentration. When the concentration is high enough, the current tends to stabilize, representing the characteristics of Michaelis-Menten kinetics. The response current varies linearly with the concentration of xanthine over the range from 7.4×10^{-7} mol L^{-1} to 7.5×10^{-5} mol L^{-1}. The regression equation of linear part of the curve is $\Delta I = 9.91 c_{xanthine} + 2.46$ ($R^2 = 0.996$). The limit of detection is 2.0×10^{-7} mol L^{-1}.

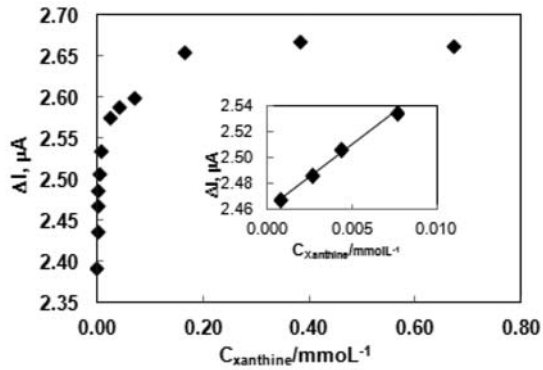

Fig. 5. Effect of xanthine concentration on the response of Fe_3O_4–CPEE (0.05 mol L^{-1}, pH 6.0 phosphate buffer, –0.20 V)

Under the optimized conditions, the amperometric response of the modified electrode to successive addition of xanthine was evaluated. The electrode showed an excellent and fast bioelectroctalytic response with 95% of the steady state current being achieved in about 15 s for xanthine. The operational stability of the enzyme electrode was measured by the same electrodes continuous response to 0.05 mol L^{-1} pH 6.0 phosphate buffer containing

0.1 mmol L^{-1} of xanthine. The RSD is 4.4% for continuous five time determinations. The long term stability of a biosensor is an important factor concerning biosensor development. In this study, the long term stability of the biosensor was investigated periodically for 7 weeks by measuring the amperometric response at a xanthine concentration of 0.1 mmol L^{-1} xanthine. During this period, the electrode was stored under dry conditions at 4 °C and measurements were performed each 3–5 days. The biosensor lost only 3.5% of the initial response after one week and %10 after 3 weeks. The response current of the biosensor decreases 29% of the initial response after 7 weeks. The decrease in the response current of the biosensor can be attributed to the time dependent loss of enzyme bioactivity. These results imply that the presented biosensor has good repeatability and long-term stability. Good long-term stability and repeatability may be attributed to the immobilization of the enzyme by cross-linking that prevents the enzyme leaking out of the carbon paste matrix.

The interferences from ascorbic acid (1×10^{-4} mol L^{-1}), uric acid (1×10^{-4} mol L^{-1}) and glucose (1×10^{-4} mol L^{-1}) in the detection of 1×10^{-4} mol L^{-1} xanthine were evaluated. The interferences of uric acid and glucose were 0.6% and 0.1%, respectively. Thus, addition of uric acid and glucose did not cause a significant interference to the detection of xanthine. For ascorbic acid, an increase of the current by 4% at the concentration of 1×10^{-4} mol L^{-1} was observed which was still reasonably small. These results indicate that detecting xanthine through the current of hydrogen peroxide reduction at the low working potential of –0.20 V provides practically interference free biosensor response.

Table 1 shows the analytical characteristics of the presented biosensor along with those reported in the literature. The proposed xanthine biosensor has the advantage of lower detection limit, high sensitivity, low working potential, and interference free sensing when compared with most of the other xanthine biosensors.

3. 5. Determination of Xanthine in Urine

The practical application of the developed biosensor was established by the determination of xanthine in human urine. The urine sample was diluted 100 times with 0.05 M pH 7.0 phosphate buffer without any other pretreatment process. The concentration of xanthine contained in the urine sample was tested using the proposed biosensor. Standard addition method was used to calculate the original xanthine concentration in urine sample. The mean xanthine concentration in the urine sample calculated from the standard addition plots was found to be 12.8 ± 0.7 μM (n = 4). To test the accuracy of the method, the urine sample was spiked with 20.5 μM standard xanthine solution and the xanthine concentration in the spiked sample was measured by Fe_3O_4–CPEE. The xanthine concentrations of the spiked samples were found to be 31.9 μM, 30.6 μM, 32.1 μM, 29.5 μM. The average % recovery of exogenously added xanthine was calculated and found to be 93.2 ± 3.6%. From these recovery values it is concluded that proposed biosensor can be used for the determination of xanthine in urine samples with an acceptable recovery.

4. Conclusion

In this study, we have presented the use of magnetite nanoparticles to develop an electrochemical xanthine biosensor. The magnetite nanoparticles increased electroactive surface area of the electrode and electron transfer at solution/electrode interface thus enhancing the sensitivity of the biosensor. The magnetite nanoparticles also allowed the determination of xanthine at a low potential (–0.20 V) hence reduce the risk of interference. The electrocatalytic detection of hydrogen peroxide has made possible the development of a highly effective and selective xanthine biosensor in the presence of easily oxidizable compounds. The cost of the biosensor is lower than that of the conventional technique and its fabrication process is very simple. The biosensor exhibits good operational and storage stability. Therefore, the presented biosensor offers a good promise for practical applications in real samples.

5. References

1. N. Arikyants, A. Sarkissian, A. Hesse, T. Eggermann, E. Leumann, B. Steinmann, *Pediatr. Nephrol.* **2007**, *22,* 310–314.
2. C. LaRosa, L. McMullen, S. Bakdas, D. Ellis, L. Krishnamurti, H.-Y. M. Wu, L. Moritz, *Pediatr. Nephrol.* **2007**, *22,* 132–135.
3. R. Devi, M. Thakur, C. S. Pundir, *Biosens. Bioelectron.* **2011**, *26,* 3420–3426.
4. X. Tang, Y. Liu, H. Hou, T. You, *Talanta* **2011**, *83,* 1410–1414.
5. R. S. Pagliarussi, L. A. P. Freitas, J. K. Bastos, *J. Sep. Sci.* **2002**, *25,* 371–374.
6. N. Cooper, R. Khosravan, C. Erdmann, J. Fiene, J. W. Lee, *J. Chromatogr. B* **2006**, *837*, 1–10.
7. G. Chen, Q. Chub, L. Zhang, J. Ye, *Anal. Chim. Acta* **2002**, *457*, 225–233.
8. J. Hlavay, S. Haemmerli, G. Gailbult, *Biosens. Bioelectron.* **1994**, *9*, 189–195.
9. J. M. Amigo, J. Coello, S. Maspoch, *Anal.Bioanal.Chem.* **2005**, *382*, 1380–1388.
10. Y. Liu, L. Nie, W. Tao, S. Ya, *Electroanalysis* **2004**, *16*, 1271–1278.
11. L. Aguí, J. Manso, P. Yáñez-Sedeño, J. M. Pingarrón, *Sensor. Actuat. B-Chem.* **2006**, *113*, 272–280.

Table 1. Characteristics of Fe_3O_4–CPEE along with those reported in the literature-

Electrode	Applied potential (V)	Detection limit (M)	Linear range (M)	Sensitivity	Repeat. (%)	Stability (days)	Response time (s)	Ref.
XO/PtMPs/PdMPs/GE	–0.05 vs. Ag/AgCl	1.5×10^{-6}	1.5×10^{-6} –7.0×10^{-5}	0.39 μA μM^{-1}	–	–	60	[17]
XO/PPy/Fc/Pt	+0.70 vs. SCE	1.0×10^{-6}	1.0×10^{-5} –4.0×10^{-4}	–	6	35% loss after 45 days	180–240	[14]
XO/ZnONPs-PPy/Pt	–0.38 vs. Ag/AgCl	8.0×10^{-7}	8.0×10^{-7} –4.0×10^{-5}	–	<5.1	40% loss after 100 days	–	[3]
XO/SC/MWCNTs/GCE	+0.40 vs. SCE	1.0×10^{-7}	2.0×10^{-7} –1.0×10^{-5}		3.4	5% loss after 90 days	6	[12]
XO-CMC-CD/ADA/Au	+0.70 vs. Ag/AgCl	2.0×10^{-4}	3.0×10^{-4} –1.0×10^{-2}	8.2 mA/Mcm^2	–	7% loss after 21 days	14	[39]
XO/DWCNT/CPE	+0.90 vs. Ag/AgCl	–	2.0×10^{-6} –5.0×10^{-5}		4.2	–	150	[40]
XO/BQ/CPE	+0.25 vs. Ag/AgCl	1.0×10^{-7}	1.9×10^{-7} –5.5×10^{-6} 5.2×10^{-5} –8.2×10^{-4}	–	3.5	34% loss after 18 days	100	[35]
XO/PVF/CPE	+0.60 vs. Ag/AgCl	1.0×10^{-7}	1.9×10^{-7} –2.1×10^{-6} 1.9×10^{-6} –1.0×10^{-5}	–	7.2	33% loss after 21 days	50	[35]
XO-ADA/SWNT/Pyr-βCD	+0.60 vs. Ag/AgCl	2.0×10^{-6}	5.0×10^{-6} –6.0×10^{-4}	5.9 mA/Mcm^2	6.1	67% loss after 30 days	10	[41]
XOD/CHIT/Fe-NPs@Au/PGE	+0.50 vs. Ag/AgCl	1.0×10^{-7}	1.0×10^{-7} –3.0×10^{-5}	0.001169 mA$\mu M^{-1}cm^{-2}$	<2.45	25% loss after 100 days	3	[42]
Fe_3O_4@APTES-CD:XO/CPE	+0.60 vs. Ag/AgCl	2.0×10^{-6}	5.0×10^{-6} –1.2×10^{-4}	130 mA/M	4.1	27% loss after 30 days	7	[43]
Fe_3O_4/APTES–PEG–XO/SWNT	+0.60 vs. Ag/AgCl	6.0×10^{-8}	2.5×10^{-7} –3.5×10^{-6}	1.31 AM^{-1} cm^{-2}	6.5	24% loss after 40 days	12	[44]
XOD/ZnO-NP/CHIT/c-MWCNT/PANI/Pt	+0.50 vs. Ag/AgCl	1.0×10^{-7}	1.0×10^{-7} –1.0×10^{-5}	–	–	30% loss after 30 days	4	[37]
Naf/XO-CD/pAuNP/SWNT/GCE	+0.65 vs. Ag/AgCl	4.0×10^{-8}	5.0×10^{-8} –9.5×10^{-6}	152 mA/M	5.2	9% loss after 40 days	9	[45]
Fe_3O_4–CPEE	–0.20 vs. Ag/AgCl	2.0×10^{-7}	7.4×10^{-7} –7.5×10^{-5}	47 μAmM cm^{-2}	4.4	29% loss after 49 days	15	This work

GE:Graphite electrode, PtMPs:platinium microparticle, PdMPs:palladium microparticle, PPy:polypyrrole, ZnONPs:zinc oxide nanoparticles, SC:-sillica sol-gel film, MWCNT:multiwall carbon nanotube, CMC-CD:β-cyclodextrin-branched carboxymethycellulose, ADA:1-adamantyl, DWCNT:double wall carbon nanotube, CPE:carbon paste electrode, BQ: 1,4-benzoquinone, PVF: poly(vinylferrocene), SWNT:single walled carbon nanotubes, Pyr-βCD: mono-6-ethylenediamino-(2-pyrene carboxamido)-6-deoxy-β-cyclodextrin, PGE:pencil graphite electrode, CHIT/Fe-NPs@Au: chitosan bound gold coated iron nanoparticles, APTES:(3-aminopropyl)triethoxysilane, CD: mono-6-formyl-b-cyclodextrin PEG: monomethoxypolyethylene glycol, c-MWCNT: carboxylated multiwalled carbon nanotube PANI:polyaniline, Naf:nafion, pAuNp: 2-mercaptoethanesulfonic acid, 1-adamantanethiol, and p-aminothiophenol modified gold nanoparticles

12. Y. Gao, C. Shen, J. Di, Y. Tu, *Mat. Sci. Eng. C* **2009**, *29*, 2213–2216.
13. Ü. A. Kirgöz, S. Timur, J. Wang, A. Telefoncu, *Electrochem. Commun.* **2004**, *6*, 913–916.
14. F. Arslan, A. Yaşar, . Kiliç, . **2006**, *34(1)*, 111–126.
15. Y. Teng, C. Chen, C. X. Zhao, H. L. Zhao, M. B. Lan, *Sci. China Chem.* **2010**, *53*, 2581–2586.
16. E. Kilinc, A. Erdem, L. Gökgünneç, T. Dalbastı, M. Karaoğlan, M. Özsöz *Electroanalysis,* **1998**, *10*, 273–275.
17. T. Dodevska, E. Horozova, N. Dimcheva, *Cent. Eur. J. Chem.* **2010**, *8(1)*, 19–27.
18. D. Shan, Y. Wang, H. Xue, S. Cosnier, *Sensor. Actuat. B-Chem.* **2009**, *136*, 510–515.
19. T. Hoshi, T. Noguchi, J. Anzai, *Mat. Sci. Eng. C* **2006**, *26*, 100–103.
20. H. S. Nakatani, L. Vieira dos Santos, C. P. Pelegrine, S. Terezinha, M. Gomes, M. Matsushita, N. Evelázio de Souza, J. Vergilio Visentainer, *Am. J. Biochem. Biotechnol.* **2005**, *1(2)*, 85–89.
21. J. Lin, L. Zhang, S. Zhang, *Anal. Biochem.* **2007**, *370*, 180–185.
22. X. Kang, Z. Mai, X. Zou, P. Cai, J. Mo, *Anal. Biochem.* **2007**, *369*, 71–79.
23. Z. Wu, L. Chen, G. Shen, R. Yu, *Sensor. Actuat. B-Chem.* **2006**, *119*, 295–301.
24. Y. Zhou, P. X. Yuan, Y. Q. Chai, C. L. Hong, *Biomaterials* **2009**, *30*, 2284–2290.
25. A. Kaushik, P. R. Solanki, A. A. Ansari, G. Sumana, S. Ahmad, B. D. Malhotra, *Sensor. Actuat. B-Chem.* **2009***, 138*, 572–580.
26. L. Yang, X. Ren, F. Tang, L. Zhang, *Biosens. Bioelectron.* **2009**, *25*, 889–895.
27. B. W. Lu, W. C. Chen, *J. Magn. Magn. Material.* **2006**, *304*, e400–e402.
28. A. J. Bard, L. R. Faulkner, *Electrochemical Methods: Fundamentals and Applications,* **2000**, New York, USA: John Wiley.
29. J. Wang, *Analytical Electrochemistry. (3.rd ed.)* **2006**, New Jersey, USA: Wiley Wch, John Wiley & Sons Inc.
30. X. Che, R. Yuan, Y. Chai, J. Li, Z. Song, W. Li, *Electrochim. Acta* **2010**, *55*, 5420–5427.
31. L. M. Rossi, A. D. Quach, Z. Rosenzweig, *Anal. Bioanal. Chem.* **2004**, *380*, 606–613.
32. F. N. Comba, M. D. Rubianes, L. Cabrera, S. Gutierrez, P. Herrasti, G. Rivas, *Electroanalysis* **2010**, *22*, 1566–1572.
33. Y. Zhang, G. Wen, Y. Zhou, S. Shuang, C. Dong, M. M. F. Choi, *Biosens. Bioelectron.* **2007**, *22*, 1791–1797.
34. L. Yang, X. Ren, F. Tang, L. Zhang, *Biosens. Bioelectron.* **2009**, *25*, 889–895.
35. P. E. Erden, Ş. Pekyardımcı, E. Kılıç, *Acta Chim. Slov*. **2012**, *59*, 824–832.
36. M. Stredansky, A. Pizzariello, S. Miertus, J. Svorc, *Anal. Biochem*. **2000**, *285*, 225–229.
37. R. Devi, S. Yadav, C. S. Pundir, *Analyst*, **2012**, *137*, 754–759.
38. A. Kumar Basu, P. Chattopadhyay, U. Roy Choudhury, R. Chakraborty, *Ind. J. Exp.Biol.* **2005,** *43*, 654–661
39. R. Villalonga, M. Matos, R. Cao, *Electrochem. Commun.* **2007**, *9*, 454–458.
40. Ü. Anık, S. Çevik, Microchim. Acta **2009**, *166*, 209–213.
41. R. Villalonga, P. Diez, M. Gamella, J. Reviejo, J.M. Pingarron, *Electroanalysis* **2011**, *23*, 1790–1796
42. R. Devi, S. Yadav, R. Nehra, S. Yadav, C. S. Pundir, *J. Food Eng.* **2013**, *115*, 207–214
43. P. Díez, R. Villalonga, M. L. Villalonga, J. M. Pingarrón, *J. Colloid Interface Sci.* **2012**, *386*, 181–188.
44. R. Villalonga, M. L.Villalonga, P. Diez, J. M. Pingarron, *J. Mater. Chem.* **2011**, *21*, 12858–12864.
45. R. Villalonga, P. Díez, M. Eguílaz, P. Martínez, J. M. Pingarrón, *ACS Appl. Mater. Interfaces* **2012**, *4*, 4312–4319

Povzetek

Razvili smo amperometrični ksantinski biosenzor na osnovi ksantin oksidaze (XO) imobilizirane na ogljikovo pasto spremenjeno z nanodelci Fe_3O_4. S ciklovoltametrijo in elektrokemijsko impedančno spektroskopijo smo proučevali prenos elektronov v nespremenjeni in z nanodelci Fe_3O_4 spremenjeni ogljikovi pasti in potrdili, da nanodelci Fe_3O_4 povečajo elektroaktivno površino elektrode in prenos elektronov na vmesniku raztopina / elektroda. Pri optimizaciji smo določili optimalne vrednosti parametrov in sicer pH 6,0, nanos nanodelcev 14,2 % in nanos encima XO 0,6 enote. Biosenzor z ogljikovo pasto spremenjeno z nanodelci Fe_3O_4 omogoča določanje ksantina pri –0,20 V, kar zmanjšuje morebitne interference spojin kot sta askorbinska in sečna kislina. Umeritvena krivulja je bila linearna v območju $7.4 \times 10^{-7} – 7.5 \times 10^{-5}$ mol L^{-1} ksantina, meja zaznave pa 2.0×10^{-7} mol L^{-1}. Biosenzor smo uspešno uporabili za določanje ksantina v urinu.